AMP-activated protein kinase: an ultrasensitive system for monitoring cellular energy charge

D. Grahame HARDIE[1], Ian P. SALT, Simon A. HAWLEY and Stephen P. DAVIES

Biochemistry Department, Dundee University, MSI/WTB Complex, Dow Street, Dundee DD1 5EH, Scotland, U.K.

The AMP-activated protein kinase cascade is activated by elevation of AMP and depression of ATP when cellular energy charge is compromised, leading to inhibition of anabolic pathways and activation of catabolic pathways. Here we show that the system responds in intact cells in an ultrasensitive manner over a critical range of nucleotide concentrations, in that only a 6-fold increase in activating nucleotide is required in order for the maximal activity of the kinase to progress from 10 % to 90 %, equivalent to a co-operative system with a Hill coefficient (*h*) of 2.5. Modelling suggests that this sensitivity arises from two features of the system: (i) AMP acts at multiple steps in the cascade (multistep sensitivity); and (ii) the upstream kinase is initially saturated with the downstream kinase (zero-order ultrasensitivity).

Key words: 5-aminoimidazole-4-carboxamide riboside, cell signalling, metabolic control, zero-order ultrasensitivity.

INTRODUCTION

AMP-activated protein kinase kinase (AMPKK) and AMP-activated protein kinase (AMPK) are the upstream and downstream components respectively of a highly conserved protein kinase cascade [1,2]. Previous studies [3–5] have shown that elevation of AMP activates the system by four mechanisms: (1) allosteric activation of AMPKK; (2) binding of AMP to AMPK, rendering it a poorer substrate for protein phosphatases; (3) binding of AMP to AMPK, making it a better substrate for the upstream kinase, AMPKK; and (4) allosteric activation of AMPK (Scheme 1). Activating effects (2) and (4) are antagonized by high (mM) concentrations of ATP [3,5], as is the activation of AMPKK by AMPK [6] although, in the latter case, it has not been tested whether this is enzyme-mediated (mechanism 1), substrate-mediated (mechanism 3), or both. The AMPK cascade is therefore activated in intact cells under conditions where AMP is elevated and ATP is depressed. Owing to the action of adenylate kinase, AMP and ATP usually change in reciprocal directions in cells, and the AMP:ATP ratio varies approximately as the square of ADP:ATP [2], making the former ratio a very sensitive indicator of cellular energy charge. In some cells, AMPK might also be inhibited by phosphocreatine [7]. The consequences of AMPK activation include inactivation of ATP-consuming, anabolic pathways, e.g. fatty acid synthesis via phosphorylation of acetyl-CoA carboxylase, and sterol synthesis via phosphorylation of 3-hydroxy-3-methylglutaryl-CoA reductase [3,8]. The system also activates at least one ATP-producing catabolic pathway, i.e. fatty acid oxidation, via depression of malonyl-CoA levels [9,10]. Experiments with the AMPK activator, 5-aminoimidazole-4-carboxamide (AICA) riboside, suggest that it might also stimulate glucose oxidation by enhancing glucose uptake [9,11]. AMPK could therefore act to match the supply of ATP to the demand for the nucleotide. It might be particularly important during periods of cellular stress associated with ATP depletion, such as treatment with heat shock or metabolic poisons in hepatocytes [12], ischaemia in heart muscle [13] and exercise or contraction in skeletal muscle [14–17].

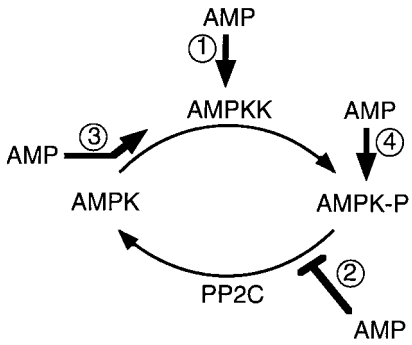

Scheme 1 The AMPK cascade is activated by AMP via four mechanisms

(1) Allosteric activation of AMPKK; (2) binding of AMP to AMPK, rendering it a poorer substrate for protein phosphatases; (3) binding of AMP to AMPK, making it a better substrate for the upstream kinase, AMPKK; and (4) allosteric activation of AMPK.

In recent years a large number of protein kinase cascades have been found, especially those involving the mitogen-activated protein (MAP) kinases and their relatives [18]. An obvious question is why some, but not all, protein kinases are arranged in cascades, with multiple cycles of phosphorylation and dephosphorylation. A number of theoretical studies [19–22] have addressed the possibility that this arrangement might produce an ultrasensitive response, defined as a response where a change from 10 % to 90 % of the maximal one requires a change in the initial signal of less than 81-fold, as is the case in a hyperbolic system [23]. Chock and Stadtman [19] pointed out that ultrasensitivity is possible when the activating signal acts at more than one step in a cascade (multistep ultrasensitivity). Goldbeter and

Abbreviations used: AICA, 5-aminoimidazole-4-carboxamide; AMPK, AMP-activated protein kinase; AMPKK, AMPK kinase; CaMK1, calmodulin-dependent protein kinase 1; CaMKK, calmodulin-dependent protein kinase kinase; MAP, mitogen-activated protein; PP2C, protein phosphatase-2C.

[1] To whom correspondence should be addressed (e-mail d.g.hardie@dundee.ac.uk).

Koshland [20] extended this analysis, and showed that the sensitivity of even a single covalent modification cycle would dramatically increase if one or both of the interconverting enzymes were operating in the zero-order region (zero-order ultrasensitivity). This latter phenomenon has been shown to be operative in protein kinase cascades reconstituted in cell-free systems [24,25], and recently in intact *Xenopus laevis* oocytes micro-injected with recombinant Mos protein kinase [26]. In the present study, we examine whether ultrasensitivity occurs in the AMPK cascade, utilizing both modelling of the system with experimentally determined parameters, and analysis of extracts from intact cells containing different concentrations of activating nucleotide.

MATERIALS AND METHODS

Reagents

AMPK, AMPKK, calmodulin-dependent protein kinase 1 (CaMK1), calmodulin-dependent protein kinase kinase (CaMKK) and protein phosphatase-2C (PP2C) were purified as described previously [4–6]. Sources of other materials have also been described previously [27,28].

Estimation of kinetic parameters

AMPK was assayed as in [29], except that the AMARA peptide (AMARAASAAALARRR) [4,30] was used in place of the SAMS peptide (HMRSAMSGLHLVKRR) (structures of the peptides are shown in parentheses in single-letter amino acid form). Reactivation of AMPK and CaMK1 by AMPKK and/or CaMKK, and inactivation of AMPK by PP2C, was performed as described previously [4,5].

Modelling

Curve fitting was performed using Kaleidagraph (Abelbeck software), and parameters derived from curve fitting are given ± S.E.M. The modelling in Figure 2 was performed using Microsoft Excel, varying the AMP concentration from 0 to 20 μM in increments of 0.4 μM. Eqn. (7) of Goldbeter and Koshland [20] was utilized, except that for mechanism 1 the V_{max} for AMPKK was multiplied by the factor [AMP]/(13 + [AMP]) (13 μM being the EC_{50} for the effect of AMP on AMPKK), for mechanism 2 the V_{max} for PP2C was multiplied by the factor (1 − [AMP])/(4 + [AMP]) (4 μM being the assumed EC_{50} for effects of AMP on AMPK), and for mechanism 3 the V_{max} for AMPKK was multiplied by [AMP]/(4 + [AMP]) (4 μM being the assumed EC_{50} for effects of AMP on AMPK).

Intact cell experiments

INS-1 cells (3×10^6) were seeded in 10-cm dishes and grown for 4–5 days in RPMI 1640 medium supplemented with 10 % (v/v) heat-inactivated fetal bovine serum/10 mM Hepes/2 mM glutamine/1 mM pyruvate/50 μM 2-mercaptoethanol/100 units · ml^{-1} penicillin and 100 μg · ml^{-1} streptomycin. The medium was removed and cells were preincubated for 60 min at 37 °C in 5 ml of KRH buffer [119 mM NaCl/20 mM sodium Hepes (pH 7.4)/10 mM glucose/5 mM $NaHCO_3$/4.75 mM KCl/1.3 mM $CaCl_2$/1.2 mM $MgSO_4$/0.1 % (w/v) BSA]. The medium was replaced with 5 ml of KRH buffer containing AICA riboside (at various concentrations between 0 and 2 mM), and incubation continued for 20 min. The medium was replaced with 0.5 ml of ice-cold lysis buffer [50 mM Tris/HCl (pH 7.4)/250 mM mannitol/50 mM NaF/1 mM sodium pyrophosphate/1 mM EDTA/1 mM EGTA/1 mM dithiothreitol/0.1 mM benzamidine/0.1 mM PMSF/5 μg · ml^{-1} soya-bean trypsin inhibitor/1 % (v/v) Triton X-100] and the lysate was scraped into a microcentrifuge tube. An aliquot (50 μl) was taken for AMPK assay, perchloric acid [5 % (v/v) final] was immediately added to the remainder, and protein-free perchloric acid extracts were prepared [3]. Nucleotides were analysed by HPLC, and AMPK was assayed in poly(ethylene glycol) precipitates [3]. Immunoprecipitation of AMPK was performed as described previously [28].

RESULTS AND DISCUSSION

Estimation of kinetic parameters

To allow us to model the system using equations derived by Goldbeter and Koshland [20], we needed to estimate a number of parameters. We have previously determined the EC_{50} for the allosteric activation of AMP on AMPK to be 4.4 ± 2.2 μM [3], whereas that for the inhibition by AMP of dephosphorylation of AMPK by PP2C was 3.1 ± 0.3 μM [5]. In Figure 1(A) we have estimated the EC_{50} for reactivation of dephosphorylated AMPK by CaMKK to be 4.3 ± 0.6 μM. We utilized CaMKK rather than AMPKK as the upstream kinase in order to eliminate any effect of AMP on it, and thus to observe only the substrate-mediated effect due to binding of AMP to AMPK [4]. We also found that this effect of AMP, as for the allosteric activation [3] and the inhibition of dephosphorylation [5], is antagonized by high (mM) concentrations of ATP. If the ATP concentration was increased from 200 μM to 2 mM, the EC_{50} increased 10-fold to ≈ 100 μM (results not shown). Since all three effects (mechanisms 1, 2 and 4 in Scheme 1) have a similar concentration-dependence on

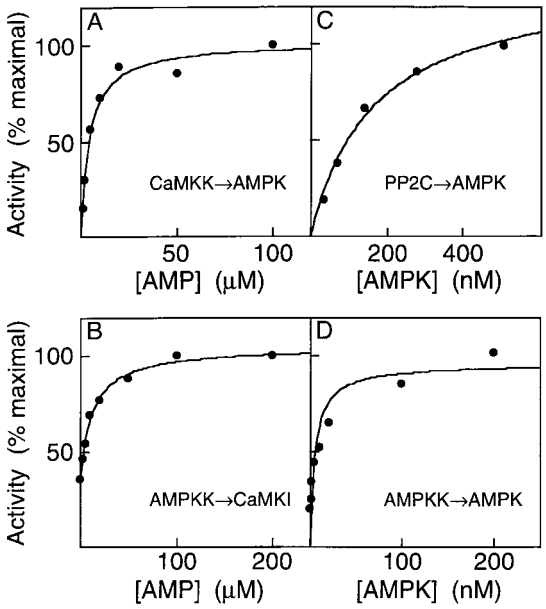

Figure 1 Determination of kinetic parameters required for modelling of the AMPK cascade

(**A**) Effect of AMP on reactivation of AMPK by CaMKK: this measures the substrate-mediated effect of AMP only; (**B**) effect of AMP on reactivation of CaMKI by AMPKK: this measures the enzyme-mediated effect of AMP only; (**C**) effect of AMPK concentration on inactivation by PP2C; (**D**) effect of AMPK concentration on reactivation by AMPKK. Data in (**A**) and (**B**) were fitted to the equation $v = \text{Basal} + V_{max} \cdot [\text{AMP}]/(EC_{50} + [\text{AMP}])$; data in (**C**) and (**D**) were fitted to the equation $v = V_{max} \cdot [\text{AMPK}]/(K_m + [\text{AMPK}])$.

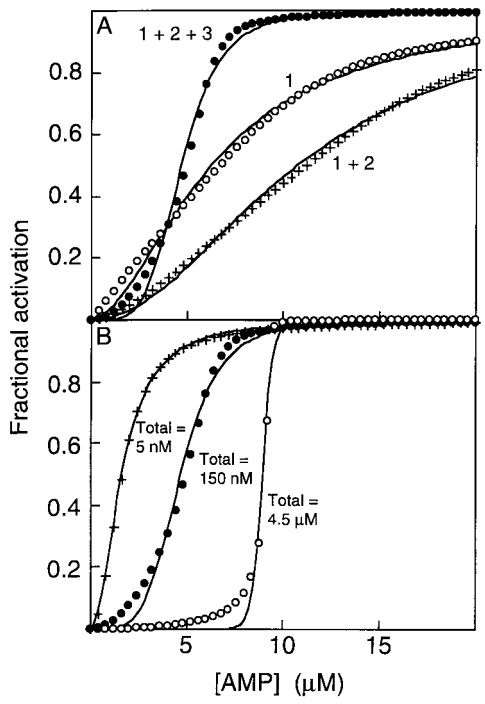

Figure 2 Modelling of the AMPK cascade

(**A**) AMP activates AMPKK only (mechanism 1; shown by open circles), AMP activates AMPKK and either inhibits dephosphorylation (mechanism 1+2; shown by crosses) or has the full three-input mechanism (mechanism 1+2 +3; shown by filled circles). (**B**) Modelling using mechanism 1+2 +3, but varying the total concentration of the kinase from 150 nM (filled circles) to 5 nM (crosses) and 4.5 μM (open circles). The symbols show values generated by the equations; the continuous lines are theoretical curves obtained by fitting of these values to the Hill equation {fractional activation = $[AMP]^h/(EC_{50h}+[AMP]^h)$}, where h is the Hill coefficient.

AMP, and all are antagonized by high ATP, the simplest hypothesis is that they are all produced by binding of AMP at a single allosteric site on AMPK. In our modelling, we have assumed the EC_{50} for AMP at this site to be 4 μM. Utilizing CaMK1 as an AMP-insensitive substrate [4], the EC_{50} for allosteric activation of the upstream kinase (AMPKK) by AMP was estimated to be 13 ± 2 μM (Figure 1B).

We also needed an estimate of the total concentration of AMPK in the cell. On the basis of the specific activity after the gel-filtration step [31], and correcting for the purity of the $\alpha\beta\gamma$ complex at this step estimated by densitometry of Coomassie-Blue-stained gels, the specific activity of the pure enzyme was estimated to be 6100 units/mg. Assuming a molecular mass for the $\alpha\beta\gamma$ complex of 140 kDa, and using a specific activity and protein concentration in post-mitochondrial supernatants from rat liver of 1 unit/mg and 30 mg/ml respectively, the concentration of AMPK in this crude fraction would be 35 nM. Allowing for the dilution with extracellular fluid and extraction buffer that occurs during homogenization, a reasonable estimate for the average intracellular concentration of AMPK in rat liver would be 150 nM. The kinase is expressed ubiquitously [32], and this parameter is unlikely to be dramatically different in other cell types.

The other two parameters we needed to estimate were the K_m of AMPKK and PP2C for phosphorylation/dephosphorylation of AMPK. These were estimated using purified, reconstituted systems (Figures 1C and 1D). Our estimate for the K_m of PP2C for AMPK (160 ± 20 nM) was comparable with our estimate of the concentration of AMPK in the cell (150 nM). However, our estimate of the K_m of AMPKK for AMPK (5.4 ± 1.4 nM) was very much lower, introducing the intriguing possibility that the system would display zero-order ultrasensitivity [20].

Modelling of the system

When modelling the system, we chose not to include the allosteric effect of AMP on the downstream kinase (mechanism 4), mainly because it is not feasible to measure this in intact cells. We utilized eqn. (7) of Goldbeter and Koshland [20]. Derivation of this equation made the assumption that the contribution of the Michaelis complexes (in this case, complexes between AMPKK and AMPK) could be ignored, but this is appropriate if binding of AMPKK to AMPK does not inhibit the latter. We consider this to be reasonable, since AMPKK co-precipitates with AMPK using antibodies raised against the latter [6], but this does not affect the kinase activity of AMPK (results not shown). Figure 2(A) shows the results obtained when the system was modelled in three different ways: (i) including only the allosteric effect of AMP on the upstream kinase (mechanism 1 in Scheme 1); (ii) also including the inhibition of dephosphorylation of the downstream kinase by AMP (mechanisms 1+2); and (iii) also including the substrate (AMPK)-mediated effect of AMP on phosphorylation by AMPKK (mechanisms 1+2+3). With mechanism 1 alone, the system gave a moderately sigmoidal response, equivalent to a co-operative system with a Hill coefficient (h) of 1.8. If AMP had two inputs (mechanisms 1+2), the response curve was shifted to the right and was slightly more sigmoidal, equivalent to $h = 2.1$. If the full three-input model was used (1+2+3), the system became much more sigmoidal, equivalent to $h = 4.6$. Figure 2(B) shows that the high Hill coefficient of the three-input model was at least partly due to zero-order ultrasensitivity, i.e. the fact that the upstream kinase was initially saturated with its substrate (K_m of 5 nM compared with a total AMPK concentration of 150 nM). If the total kinase concentration was increased in the model by 30-fold to 4.5 μM, the curve became even more sigmoidal with $h = 34$, the system now almost becoming a digital on–off switch. If the total kinase concentration was decreased in the model by 30-fold to 5 nM (i.e. becoming equal to the K_m value), the curve became less sigmoidal with $h = 2.1$.

The EC_{50} values for the effects of AMP on AMPK and AMPKK used in Figure 1 were determined at 200 μM ATP. At 10-fold higher ATP concentrations, the EC_{50} for the effect of AMP on AMPK increases by about 10-fold ([3,5]; also see the previous section of the Results and Discussion). If we used an EC_{50} for the effect of AMP on AMPK of 40 μM rather than 4 μM in the simulation, using the full three-input model (mechanism 1+2+3) the curve shifted to the right (results not shown). The half-maximal effect of AMP now occurred at a concentration of 21 μM rather than 4.7 μM, but there was little change in the shape of the curve (h of 3.7 compared with 4.6). It is not yet clear whether high concentrations of ATP also antagonize the effects of AMP on the upstream kinase, AMPKK (for technical reasons this is currently difficult to study). However, if we increased the EC_{50} for the effects of AMP on both AMPK and AMPKK by a factor of 10 (to 40 and 130 μM respectively), the half-maximal effect of AMP increased from 5 to 47 μM, while the Hill coefficient h was almost the same (4.4 compared with 4.7). Increasing the ATP concentration used in the simulation therefore causes the curve to shift towards the right, but does not markedly change the sensitivity of the system.

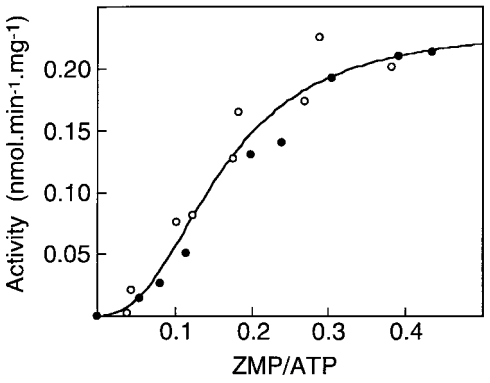

Figure 3 Ultrasensitivity of the AMPK system in intact INS-1 cells

In order to correct for minor differences in nucleotide recovery between different samples, results are expressed as ZMP:ATP ratios. Each data point represents the ZMP:ATP ratio and AMPK activity from a single dish: open and filled circles are from experiments performed on different days. The pooled data were fitted to the Hill equation $\{v = V_{max} \cdot [ZMP/ATP]^h/(EC_{50h} + [ZMP/ATP]^h)\}$, where h is the Hill coefficient.

The only parameters required for the modelling that could not be readily estimated were the maximal velocities for AMPKK and the protein phosphatase, and these were set arbitrarily to unity. Increasing the V_{max} for AMPKK 5-fold relative to the protein phosphatase shifted the curve to the left (with a decrease in EC_{50} from 4.7 to 1.9 μM) and moderately increased the sensitivity (h from 4.6 to 4.9), presumably because this accentuates the effect of the upstream kinase, which is operating under zero-order conditions. Conversely, increasing the V_{max} for the protein phosphatase 5-fold relative to that for AMPKK shifted the curve to the right (with an increase in EC_{50} from 4.7 to 13 μM) and decreased the sensitivity moderately (h from 4.6 to 3.8). The maximal velocities of the upstream kinase and the phosphatase must be of comparable magnitude in the intact cell, otherwise AMPK would remain permanently in either the active or inactive state.

The curves shown by filled circles in Figures 2(A) and 2(B), which represent the modelled response using the full three-input model, and our best estimate for the total concentration of AMPK in the cell, have a characteristic and interesting shape. An increase from 0 to 2.3 μM AMP produces only 10% of the maximal response. Above this 'threshold', only a 3-fold change in AMP (from 2.3 to 7.0 μM) is required to progress from 10% to 90% of the maximal response, as opposed to the 81-fold change required for a hyperbolic system. The system thus responds in an ultrasensitive manner over a narrow window of critical AMP concentrations. The curve is not symmetrical, as can be seen by the imperfect fit to the Hill equation. The sharp 'off' transition at high AMP concentration occurs because the effect of the upstream kinase (which is operating at near-zero-order kinetics) dominates at high [AMP], where it is stimulated by both substrate- and enzyme-mediated effects, while the protein phosphatase is inhibited. The more gradual 'on' transition at low AMP concentration occurs because the effect of the phosphatase (which is operating nearer to first-order kinetics) dominates at low [AMP], where it is less inhibited, while the upstream kinase is only slightly active. The analyses in Figure 2 do not take into account either the allosteric activation of AMPK by AMP or the effect of the decreased ATP that usually accompanies AMP elevation in intact cells. We chose not to model these features, because their effects could not be readily assessed in the intact cell studies described below. However, if anything, these additional factors would be expected to increase the sensitivity even further.

AMP concentrations in unstressed cells are too low to measure by ^{31}P-NMR spectroscopy, so there are no reliable estimates for the concentration of free AMP in the cell. The total content of AMP in unstressed cells is typically around 50-fold lower than that of ATP (e.g. see [12]). Assuming the cellular (cytoplasmic) concentration of ATP to be 5 mM, the average total concentration of AMP in the cell would therefore be around 100 μM. However, this ignores the possibility that a large proportion of measured AMP might be bound to protein, and that some might be distributed in cellular compartments other than the cytoplasm. What is clear is that, under stress conditions where the total cellular content of AMP varies, the activation state of AMPK varies in concert with it [12,13,15,28]. In fact, measurement of the activation state of AMPK could be regarded as one of the best available methods to detect changes in the concentration of free cytoplasmic AMP, although it would remain difficult to convert kinase activity measurements into absolute concentrations of AMP.

Assessment of sensitivity in intact cells

To investigate whether the AMPK is indeed activated in an ultrasensitive manner in intact cells, we utilized the nucleoside AICA riboside. AICA riboside is converted intracellularly into a monophosphorylated form, ZMP [3,8], which mimics all of the effects of AMP on the system *in vitro* ([3]; S. A. Hawley and D. G. Hardie, unpublished work). The use of AICA riboside has two advantages over a treatment that would change the intracellular concentration of AMP. First, ZMP is about 50-fold less potent than AMP as an activator of AMPK [3,33], and therefore its cellular content is easier to measure over the range of concentrations where it causes activation. Secondly, treatments that change cellular AMP levels also affect ATP, owing to a displacement of adenylate kinase; however, ZMP is not a substrate for adenylate kinase, and so incubation of cells with AICA riboside elevates ZMP without affecting ATP [3,8]. This allowed us to use a simpler model where the effect of changes in ATP did not need to be taken into account.

We chose INS-1 cells for these analyses, because initial experiments demonstrated that incubation of these cells with AICA riboside produced a constant elevated kinase activity 15–30 min after addition. In other cells, such as isolated rat hepatocytes and adipocytes, activation by AICA riboside is more transient and does not reach an apparent steady state [3]. We incubated INS-1 cells with different concentrations of AICA riboside for 20 min, and prepared extracts from the same cells to determine AMPK activity (Figure 3) and nucleotide levels (Figures 3 and 4). Incubation with AICA riboside caused an accumulation of ZMP with no evident change in AMP, ADP or ATP (Figure 4). The ATP content was constant at 0.22 ± 0.3 μmol/mg of protein (mean $\pm$ S.E.M. for 18 measurements). The ZMP content varied from being undetectable in cells incubated without AICA riboside, to a concentration of up to 0.11 μmol/mg of protein in cells incubated with 1 mM AICA riboside. With these short incubation times, there was also no measurable formation of the triphosphorylated derivative of AICA riboside, ZTP, which elutes just after ATP [3]. The increased activity produced by AICA riboside could be completely depleted using a mixture of anti-(AMPK α1) and anti-(AMPK α2) antibodies (where α1 and α2 are subunits) [34], showing that it was entirely due to AMPK. A basal activity of

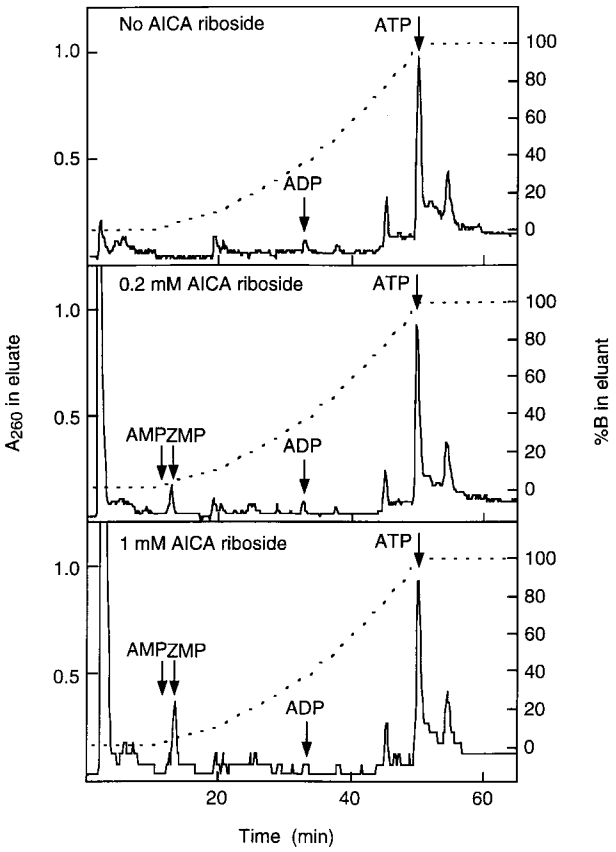

Figure 4 HPLC analysis of cellular nucleotides in INS-1 cells incubated with different concentrations of AICA riboside

Cells were incubated without AICA riboside (top panel), or with 0.2 mM (middle) or 1 mM (bottom) AICA riboside for 20 min, before nucleotide extraction and analysis. The elution times of ZMP, ADP and ATP were determined using standards. Using this gradient, ZTP elutes 1 to 2 min after ATP [3].

0.24 nmol·min^{-1}·mg^{-1} was not sensitive to the antibody and has been subtracted before plotting the data in Figure 3. Figure 3 shows that AMPK activity displayed a markedly sigmoidal response to elevation of ZMP in the INS-1 cells, equivalent to a co-operative system with a Hill coefficient h of 2.5 ± 0.5. Only a 6-fold increase in ZMP was required to produce a change from 10% to 90% of maximal response. The AMP concentration in the cells was too low to measure accurately; however, since ZMP caused a sigmoidal response, this must have been well below the EC_{50} for its effects on AMPK and AMPKK.

The AMPK cascade therefore exhibits an ultrasensitive response to elevation of the activating nucleoside monophosphate in intact cells. Although, for technical reasons, ZMP was utilized as the activating nucleotide in the intact cell experiments (Figure 3), it mimics all of the effects of AMP shown in Scheme 1 (albeit with lower potency) and the system would therefore also exhibit a sigmoidal response to the natural activator. Small fluctuations in basal AMP would have relatively little effect, but if AMP rose above a critical 'threshold' (coupled to a simultaneous fall in ATP) the system would become activated, and would initiate its effects on anabolism and catabolism. This type of response would seem quite appropriate for a system which is acting as a cellular 'fuel gauge' [1]. Our modelling suggests that the ultrasensitivity arises from at least two factors: (i) the primary signal acts at more than one step in the cascade, i.e. activating the upstream kinase, and promoting phosphorylation/inhibiting dephosphorylation by binding to the downstream kinase (multistep ultrasensitivity) [19]; and (ii) under basal conditions, the upstream kinase is saturated with the downstream kinase (zero-order ultrasensitivity) [20]. Until recently, these phenomena had only been studied by modelling [19,20] or in reconstituted cell-free systems [24,25]. While the present study was in progress, Ferrell and Machleder reported, using micro-injection of recombinant Mos in *Xenopus* oocytes [26], that the MAP kinase cascade behaves in an ultrasensitive manner. However, in their experiments, the extreme sensitivity ($h = 42$, resulting in a switch-like, 'all-or-nothing' response) was at least partly due to a positive feedback effect, which required active protein synthesis and for which the molecular mechanism was unclear [26].

This study was supported by a Programme Grant from the Wellcome Trust, and a Project Grant from the Medical Research Council. We are very grateful to Guy Rutter (University of Bristol) for supplying us with INS-1 cells, and to Art Edelman (New York University at Buffalo, U.S.A.) for supplying CaMK1 and CaMKK. We also thank Daniel Koshland for helpful comments on the manuscript.

REFERENCES

1 Hardie, D. G. and Carling, D. (1997) Eur. J. Biochem. **246**, 259–273
2 Hardie, D. G., Carling, D. and Carlson, M. (1998) Annu. Rev. Biochem. **67**, 821–855
3 Corton, J. M., Gillespie, J. G., Hawley, S. A. and Hardie, D. G. (1995) Eur. J. Biochem. **229**, 558–565
4 Hawley, S. A., Selbert, M. A., Goldstein, E. G., Edelman, A. M., Carling, D. and Hardie, D. G. (1995) J. Biol. Chem. **270**, 27186–27191
5 Davies, S. P., Helps, N. R., Cohen, P. T. W. and Hardie, D. G. (1995) FEBS Lett. **377**, 421–425
6 Hawley, S. A., Davison, M., Woods, A., Davies, S. P., Beri, R. K., Carling, D. and Hardie, D. G. (1996) J. Biol. Chem. **271**, 27879–27887
7 Ponticos, M., Lu, Q. L., Morgan, J. E., Hardie, D. G., Partridge, T. A. and Carling, D. (1998) EMBO J. **17**, 1688–1699
8 Henin, N., Vincent, M. F., Gruber, H. E. and Van den Berghe, G. (1995) FASEB J. **9**, 541–546
9 Merrill, G. M., Kurth, E., Hardie, D. G. and Winder, W. W. (1997) Am. J. Physiol. **273**, E1107–E1112
10 Velasco, G., Geelen, M. J. H. and Guzman, M. (1997) Arch. Biochem. Biophys. **337**, 169–175
11 Hayashi, T., Hirshman, M. F., Kurth, E. J., Winder, W. W. and Goodyear, L. J. (1998) Diabetes **47**, 1369–1373
12 Corton, J. M., Gillespie, J. G. and Hardie, D. G. (1994) Curr. Biol. **4**, 315–324
13 Kudo, N., Barr, A. J., Barr, R. L., Desai, S. and Lopaschuk, G. D. (1995) J. Biol. Chem. **270**, 17513–17520
14 Winder, W. W. and Hardie, D. G. (1996) Am. J. Physiol. **270**, E299–E304
15 Rasmussen, B. B. and Winder, W. W. (1997) J. Appl. Physiol. **83**, 1104–1109
16 Hutber, C. A., Hardie, D. G. and Winder, W. W. (1997) Am. J. Physiol. **272**, E262–E266
17 Vavvas, D., Apazidis, A., Saha, A. K., Gamble, J., Patel, A., Kemp, B. E., Witters, L. A. and Ruderman, N. B. (1997) J. Biol. Chem. **272**, 13255–13261
18 Blumer, K. J. and Johnson, G. L. (1994) Trends Biochem. Sci. **19**, 236–240
19 Chock, P. B. and Stadtman, E. R. (1977) Proc. Natl. Acad. Sci. U.S.A. **74**, 2766–2770
20 Goldbeter, A. and Koshland, D. E. (1981) Proc. Natl. Acad. Sci. U.S.A. **78**, 6840–6844
21 Ferrell, Jr., J. E. (1996) Trends Biochem. Sci. **21**, 460–466
22 Kholodenko, B. N., Hoek, J. B., Westerhoff, H. V. and Brown, G. C. (1997) FEBS Lett. **414**, 430–434
23 Koshland, D. E., Goldbeter, A. and Stock, J. B. (1982) Science **217**, 220–225
24 Meinke, M. H. and Edstrom, R. D. (1991) J. Biol. Chem. **266**, 2259–2266
25 Huang, C. Y. and Ferrell, Jr., J. E. (1996) Proc. Natl. Acad. Sci. U.S.A. **93**, 10078–10083
26 Ferrell, Jr., J. E. and Machleder, E. M. (1998) Science **280**, 895–898
27 Salt, I. P., Celler, J. W., Hawley, S. A., Prescott, A., Woods, A., Carling, D. and Hardie, D. G. (1998) Biochem. J. **334**, 177–187

28 Salt, I. P., Johnson, G., Ashcroft, S. J. H. and Hardie, D. G. (1998) Biochem. J. **335**, 533–539
29 Davies, S. P., Carling, D. and Hardie, D. G. (1989) Eur. J. Biochem. **186**, 123–128
30 Dale, S., Wilson, W. A., Edelman, A. M. and Hardie, D. G. (1995) FEBS Lett. **361**, 191–195
31 Davies, S. P., Hawley, S. A., Woods, A., Carling, D., Haystead, T. A. J. and Hardie, D. G. (1994) Eur. J. Biochem. **223**, 351–357
32 Stapleton, D., Mitchelhill, K. I., Gao, G., Widmer, J., Michell, B. J., Teh, T., House, C. M., Fernandez, C. S., Cox, T., Witters, L. A. and Kemp, B. E. (1996) J. Biol. Chem. **271**, 611–614
33 Henin, N., Vincent, M. F. and Van den Berghe, G. (1996) Biochim. Biophys. Acta **1290**, 197–203
34 Woods, A., Salt, I., Scott, J., Hardie, D. G. and Carling, D. (1996) FEBS Lett. **397**, 347–351

Received 30 September 1998/10 December 1998; accepted 11 January 1999